Author/s:
Wilson, KR;Macri, C;Villadangos, JA;Mintern, JD

Title:
Constitutive Flt3 signaling impacts conventional dendritic cell function

Date:
2024-07-01

Citation:
Wilson, K. R., Macri, C., Villadangos, J. A. & Mintern, J. D. (2024). Constitutive Flt3 signaling impacts conventional dendritic cell function. Immunology and Cell Biology, 102 (6), pp.500-512. https://doi.org/10.1111/imcb.12757.

Persistent Link:
https://hdl.handle.net/11343/351394

Immunology & Cell Biology 2024; **102**: 500–512
www.wileyonlinelibrary.com/journal/icb

ORIGINAL ARTICLE

OPEN

Constitutive Flt3 signaling impacts conventional dendritic cell function

Kayla R Wilson[1], Christophe Macri[1], Jose A Villadangos[1,2] & Justine D Mintern[1]

1 Department of Biochemistry and Pharmacology, The University of Melbourne, Bio21 Molecular Science and Biotechnology Institute, 30 Flemington Road, Parkville, VIC, Australia
2 Department of Microbiology and Immunology, Peter Doherty Institute for Infection and Immunity, The University of Melbourne, Parkville, VIC, Australia

Keywords
antigen presentation, dendritic cells, Flt3, ITD

Correspondence
Justine D Mintern, Department of Biochemistry and Pharmacology, The University of Melbourne, Bio21 Molecular Science and Biotechnology Institute, 30 Flemington Road, Parkville, VIC 3010, Australia.
E-mail: jmintern@unimelb.edu.au

Received 11 March 2024;
Revised 8 April 2024;
Accepted 9 April 2024

doi: 10.1111/imcb.12757

Immunology & Cell Biology 2024; **102**: 500–512

Abstract

The development of dendritic cells (DCs) depends on signaling via the FMS-like tyrosine kinase 3 (Flt3) receptor. How Flt3 signaling impacts terminally differentiated DC function is unknown. This is important given the increasing interest in exploiting Flt3 for vaccination and tumor immunotherapy. Here, we examined DCs in mice harboring constitutively activated Flt3 (Flt3-ITD). $Flt3^{ITD/ITD}$ mice possessed expanded splenic DC subsets including plasmacytoid DC, conventional DC (cDC)1, cDC2, double positive (DP) cDC1 ($CD11c^+$ $CD8^+$ $CD11b^-$ $CD103^+$ $CD86^+$), noncanonical (NC) cDC1 ($CD11c^+$ $CD8^+$ $CD11b^-$ $CD103^-$ $CD86^-$) and single positive (SP) cDC1 ($CD11c^+$ $CD8^+$ $CD11b^-$ $CD103^-$ $CD86^+$). Outcomes of constitutive Flt3 signaling differed depending on the cDC subset examined. In comparison with wild type (WT) DCs, all $Flt3^{ITD/ITD}$ cDCs displayed an altered surface phenotype with changes in costimulatory molecules, major histocompatibility complex class I (MHC I) and II (MHC II). Cytokine secretion patterns, antigen uptake, antigen proteolysis and antigen presenting function differed between WT and $Flt3^{ITD/ITD}$ subsets, particularly cDC2. In summary, Flt3 signaling impacts the function of terminally differentiated cDCs with important consequences for antigen presentation.

INTRODUCTION

FMS-like tyrosine kinase 3 (Flt3) is expressed on hematopoietic progenitors and terminally differentiated dendritic cells (DCs). The receptor binds to Flt3 ligand (Flt3L) which is produced by hematopoietic and non-hematopoietic tissues, with $CD4^+$ T cells known to secrete high amounts.[1] Upon Flt3L stimulation, Flt3 is activated (phosphorylated) and signals via the mitogen-activated protein kinase (MAPK),[2] phosphatidylinositol 3 kinase (PI3K)[3] and signal transducers and activators of transcription 3 (STAT3) pathways.[4] Flt3-dependent activation of these pathways is critical for DC generation.[3–5] When administered to mice[6,7] or humans,[8,9] Flt3L expands DCs and their progenitors. Conversely, mice lacking Flt3 ($Flt3^{-/-}$)[10] or Flt3L ($Flt3L^{-/-}$)[11] have significant defects in hematopoiesis with reduced DCs observed.[7,11,12] While the role of Flt3 in DC differentiation is well established why terminally differentiated DCs retain their high expression of Flt3 remains a curiosity. Given Flt3L is constitutively present, albeit at low levels,[13] how Flt3/Flt3L signaling impacts DC function, in particular antigen presentation, is of interest. Flt3 is proposed to regulate cDC division,[7] bone marrow-derived DC survival[14] and the expression of stimulatory genes in tumor-infiltrating conventional DC1 (cDC1).[15] Given the increasing interest in the manipulation of Flt3/Flt3L in the context of vaccination and tumor immunotherapy,[16] it is important to understand how Flt3 signaling impacts terminally differentiated DCs.

One approach to investigate how Flt3 signaling impacts DC function is to examine DCs with constitutive Flt3 signaling. The Flt3-internal tandem duplication

(Flt3-ITD) mutation leads to constitutive ligand-independent receptor activation[17–21] and occurs in approximately 20% of patients with acute myeloid leukemia (AML).[22–24] $Flt3^{ITD/ITD}$ mice develop splenomegaly, leukocytosis and monocytosis attributed to increased survival and cell cycling of bone marrow progenitor cells.[21] $Flt3^{ITD/ITD}$ and $Flt3^{+/ITD}$ mice have cell-intrinsic gene-dosage dependent increases in cDCs, plasmacytoid DCs (pDC) and DC progenitors.[25] Analysis of $Flt3^{ITD/+}$ mice suggests these DCs exhibit a gene expression profile indicative of immune tolerance.[25] However, this has yet to be confirmed by functional studies. $Flt3^{ITD/+}$ mice also possess expanded numbers of noncanonical (NC) cDC. These cells, also known as "Cx_3CR1^+ $CD8^+$" or "CD8 look-alike" DCs,[25–27] have characteristics of cDC and pDCs and have been identified in humans as "Axl^+ $Siglec6^+$ (AS DC/DC5)"[28] and "pre-DC".[29] Murine NC DCs are a population within transitional DCs (tDC) that share a continuum of phenotypes associated with pDCs and cDC2.[30] In humans, NC cDCs stimulate allogenic T cells;[28,29] however, little is known about their antigen presentation capacity.

Here, we have performed an in-depth analysis of DCs isolated from $Flt3^{ITD/ITD}$ mice and addressed how constitutive Flt3 signaling impacts DC antigen presentation capacity and function. Constitutive Flt3-ITD signaling results in altered DC function. DCs isolated from $Flt3^{ITD/ITD}$ mice have altered populations with changes in the display of cell surface molecules, cytokine secretion, antigen uptake, proteolysis and endosomal pH culminating in significant alterations in antigen presentation.

RESULTS

Flt3 expression by wild type splenic DCs

Before investigating the impact of constitutive Flt3 signaling in DCs, we first investigated the expression and regulation of the Flt3 receptor in primary DCs. In agreement with previous studies,[31] cell-surface Flt3 was detected on splenic cDC1, cDC2 and pDC, but not T or B lymphocytes. The highest expression was observed on cDC1 that are known to expand preferentially in response to Flt3L[32,33] (Figure 1a). Total Flt3 protein expression was determined for purified cell populations with two forms of Flt3 detected by immunoblotting, similar to non-DC cell lines[34,35] (Figure 1b; Supplementary figure 1a). The higher molecular weight (MW, approximately 160 kDa) species is likely cell surface Flt3, given its slower migration due to being highly glycosylated. The lower MW (approximately 130 kDa) band is likely intracellular Flt3.[34,35] Flt3 was only detected by immunoblot in cells displaying it at the cell surface; cDC1, cDC2 and pDC. The detected pattern of Flt3 varied between DC populations, with pDC expressing a higher MW species of cell surface Flt3 than cDC1 or cDC2. To determine if terminally differentiated cDC are responsive to Flt3L, primary murine splenic cDCs were isolated and stimulated with Flt3L (100 ng mL^{-1}) for 1 h. Cell surface Flt3 expression was significantly reduced on both cDC subsets following *in vitro* Flt3L stimulation (Figure 1c).

Next, Flt3 expression during cDC activation was characterized. Splenic cDCs were purified and activated *in vitro* with toll-like receptor 9 (TLR9) agonist CpG 1668 ODN (class B, 0.5 μM). Flt3 protein, detected by immunoblotting, showed an increase in intensity for higher MW Flt3, and a loss of lower MW Flt3, following CpG treatment (Figure 1d; Supplementary figure 1b). In agreement, elevated surface Flt3 was detected by flow cytometry (Figure 1e). To investigate if this were also the case following cDC activation *in vivo*, mice were injected intravenously (IV) with CpG (0.2 μM) or PBS. cDCs were purified 1 day later and Flt3 expression determined by flow cytometry (Figure 1f). In contrast to *in vitro* DC activation, a significant reduction in cell surface Flt3 was observed. Similar results were observed when DCs were isolated from mice IV injected with LPS (3 μg) or poly I:C (50 μg) (Supplementary figure 1c). A short time course, with spleens harvested from mice 0–4 h after CpG IV injection showed surface Flt3 loss by cDC1 as rapidly as 1 h after CpG administration, while cDC2 displayed the first signs of surface Flt3 reduction 4 h following CpG administration (Figure 1g). For both *in vitro* and *in vivo* treatment with CpG, increased CD86 was used as a positive control for cDC activation (Supplementary figure 1d). Together, these data demonstrate that splenic DCs express and regulate Flt3 at steady-state and during activation *in vitro* and *in vivo*. The contrast in Flt3 expression between *in vitro* and *in vivo* activation is likely due to Flt3L-dependent receptor internalization following CpG treatment *in vivo*. This is not observed *in vitro* due to limited Flt3L and therefore receptor internalization.

Flt3-ITD expands canonical and noncanonical splenic DC populations

Dendritic cell populations were analyzed in $Flt3^{+/+}$ and $Flt3^{ITD/ITD}$ littermates. Three cDC1 subpopulations were analyzed: $CD103^-$ $CD86^-$ (hereafter referred to as noncanonical "NC cDC1")[26], $CD103^+$ $CD86^+$ ("DP cDC1") and $CD103^-$ $CD86^+$ ("SP cDC1"), in addition to cDC2. All DCs were significantly increased in $Flt3^{ITD/ITD}$

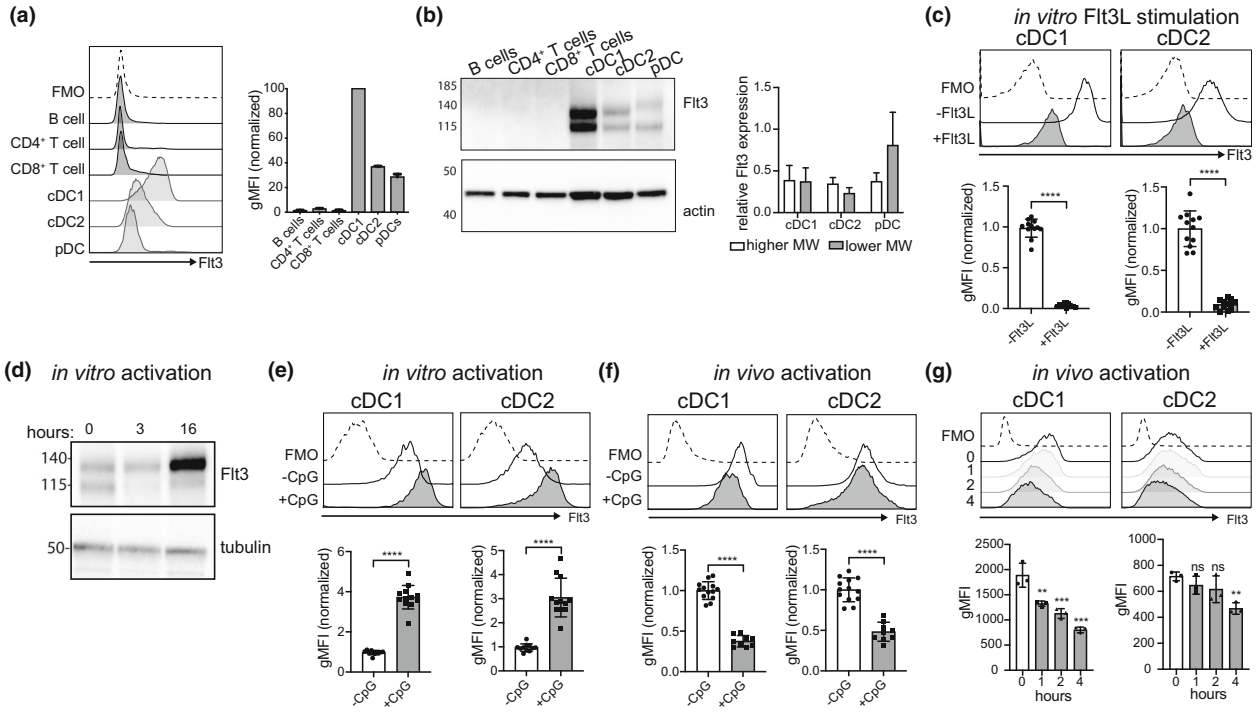

Figure 1. Flt3 expression by splenic DCs. **(a)** Representative histograms and quantification of surface Flt3 on splenocytes as determined by flow cytometry. Data are collated from two independent experiments, with cells isolated from two pooled spleens in each. The gMFI has been normalized to the maximum signal for each cell type. Bars are mean + SEM. **(b)** Purified cells were analyzed by immunoblotting and probed with anti-Flt3 (A2F10) or anti-Actin (A5060) antibodies. Blot is representative of three independent experiments. Band intensities of the higher molecular weight (MW) species and lower MW Flt3 were quantified relative to Actin. Bars are mean + SEM. **(c)** Splenic cDCs were isolated and stimulated with (+) or without (–) Flt3L (100 ng mL^{-1}) for 1 h at 37°C. Flt3 surface expression was determined by flow cytometry. Histograms are representative of three independent experiments. Symbols represent individual mice. Bars are mean ± SD, unpaired *t*-test. ****$P < 0.0001$ **(d)** Splenic cDCs were isolated and stimulated for 0, 3 or 16 h with CpG 1668 ODN (0.5 μM) at 37°C. Cell lysates were examined by immunoblotting and probing with anti-Flt3 (A2F10) or anti-tubulin (DM1A) antibodies. Blot is from one experiment. **(e)** Splenic cDCs were isolated and stimulated overnight with (+) or without (–) CpG 1668 ODN (0.5 μM) at 37°C. **(f)** Mice were injected intravenously with PBS (-CpG) or CPG 1668 ODN (0.2 μM) and spleens were harvested 1 day later or **(g)** at indicated times. **(e–g)** Surface expression of Flt3 was determined by flow cytometry. Histograms show representative surface expression. Symbols represent individual mice. **(e, f)** Data are from at least three independent experiments with the gMFI signal normalized to the maximum gMFI signal. Bars are mean ± SD, unpaired *t*-test, ****$P < 0.0001$. **(g)** Data are from one experiment. Bars are mean ± SD, one-way ANOVA with Dunnett's multiple comparisons test. ***$P < 0.001$; **$P < 0.01$, ns not significant.

mice, in agreement with previous studies[25] (Figure 2a). Specifically, $Flt3^{ITD/ITD}$ cDC1, cDC2 and pDC were expanded 8.3, 4.1 and 4.2-fold, respectively. For $Flt3^{ITD/ITD}$ cDC1 populations, a 12.8-fold increase in NC cells, a 14.8-fold increase in DP cDC1 and a 2.7-fold increase in SP cDC1 were observed. A gene-dosage dependent decrease in surface Flt3 was detected for $Flt3^{ITD/ITD}$ cDC1, cDC2 and pDC[25,35] (Figure 2b). Total Flt3 protein and Flt3 tyrosine phosphorylation status was examined following *in vitro* Flt3L (100 ng mL^{-1}) stimulation and Flt3 immunoprecipitation. Increased Flt3 tyrosine phosphorylation was observed for surface (higher MW) Flt3 in $Flt3^{+/+}$ and $Flt3^{+/ITD}$ cDCs at 10 and 30 min. $Flt3^{+/ITD}$ and $Flt3^{ITD/ITD}$ cDCs exhibited ligand-independent tyrosine phosphorylation of intracellular (lower MW) Flt3 in the absence of Flt3L. In addition, only intracellular Flt3 exhibited tyrosine phosphorylation in $Flt3^{ITD/ITD}$ cDCs (Figure 2c, Supplementary figure 2).

Flt3-ITD alters the cell surface phenotype of splenic cDCs

To characterize how constitutive Flt3 signaling impacts cDC function, cell surface levels of classical DC markers were investigated. Integrins or adhesion molecules

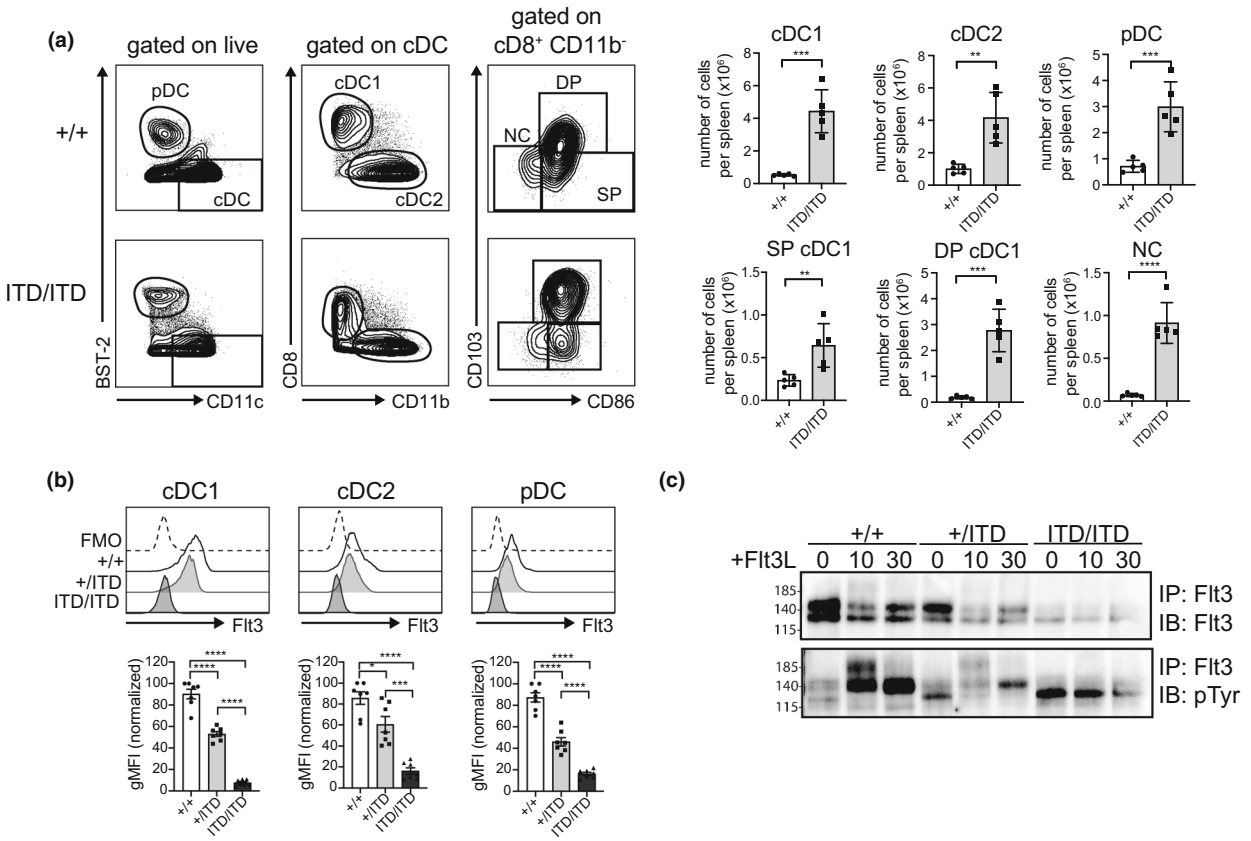

Figure 2. Flt3-ITD expands splenic DC populations. **(a)** Representative gating used to identify Flt3$^{+/+}$ and Flt3$^{ITD/ITD}$ splenic pDC (BST-2^{+} CD11c^{int}), cDC1 (CD11c^{+} CD8^{+} CD11b^{-}), cDC2 (CD11c^{+} CD8^{-} CD11b^{+}), DP cDC1 (CD11c^{+} CD8^{+} CD11b^{-} CD103^{+} CD86^{+}), NC cDC1 (CD11c^{+} CD8^{+} CD11b^{-} CD103^{-} CD86^{-}) and SP cDC1 (CD11c^{+} CD8^{+} CD11b^{-} CD103^{-} CD86^{+}). Quantification of Flt3$^{+/+}$ and Flt3$^{ITD/ITD}$ splenic DC populations. Symbols represent individual mice; data are from one experiment. Bars represent mean ± SEM, unpaired *t*-test, ****$P < 0.0001$; ***$P < 0.001$; **$P < 0.01$. **(b)** Splenic DC were isolated from Flt3$^{+/+}$, Flt3$^{+/ITD}$ and Flt3$^{ITD/ITD}$ littermates and surface Flt3 expression was determined by flow cytometry. Data are pooled from two independent experiments, with symbols representing individual mice. gMFI has been normalized to the maximum signal for each cell type. Bars represent mean ± SEM, one-way ANOVA with Dunnett's multiple comparisons test, ****$P < 0.0001$; ***$P < 0.001$; *$P < 0.05$. **(c)** Spleens from Flt3$^{+/+}$, Flt3$^{+/ITD}$ and Flt3$^{ITD/ITD}$ littermates were harvested and cDCs isolated. Cells were stimulated with Flt3L (100 ng mL^{-1}) for the indicated times at 37°C. Cells were lysed and Flt3 was subsequently immunoprecipitated using anti-Flt3 antibody (A2F10). Immunoprecipitates were analyzed by immunoblot probed with anti-Flt3 (A2F10) or anti-phospho-tyrosine (4G10) antibodies. The blot is representative of two independent repeats.

(CD11c, CD11b, CD103, CD24), phenotypic molecules (CD8), inhibitory receptors (signal-regulatory protein α, SIRPα), MHC molecules (MHC I and II), costimulatory molecules (CD86, CD80, CD40 and CD24), co-inhibitory molecules (PD-L1), chemokine receptors (XCR1) and endocytic receptors (DEC205, Clec9A, Clec12A) were analyzed (Figure 3; Supplementary figure 3). Significantly increased surface expression of MHC I, MHC II, CD103 was observed on most Flt3$^{ITD/ITD}$ cDC subsets. This was accompanied by lower CD11c, CD8, Clec9A, DEC205 and PD-L1 and varied expression of Clec12A. While Flt3$^{+/+}$ cDC2 do not express Clec12A, it was detected at the surface of Flt3$^{ITD/ITD}$ cDC2. Confirming genetic profiling of Flt3$^{+/+}$ NC cDC1s,[26] these cells had reduced surface CD103, DEC205 and CD86, in addition to reduced Clec9A, MHC II and CD40 in comparison with other Flt3$^{+/+}$ cDC subsets.

Flt3-ITD impacts DC function

For efficient T cell priming, DCs present antigen on MHC molecules (signal 1) in the presence of costimulatory molecules (signal 2) and cytokines (signal 3). Given we observed changes in signal 2 (Figure 3), we next focused on signal 1 and signal 3. Antigen presentation first requires DCs to capture antigen and

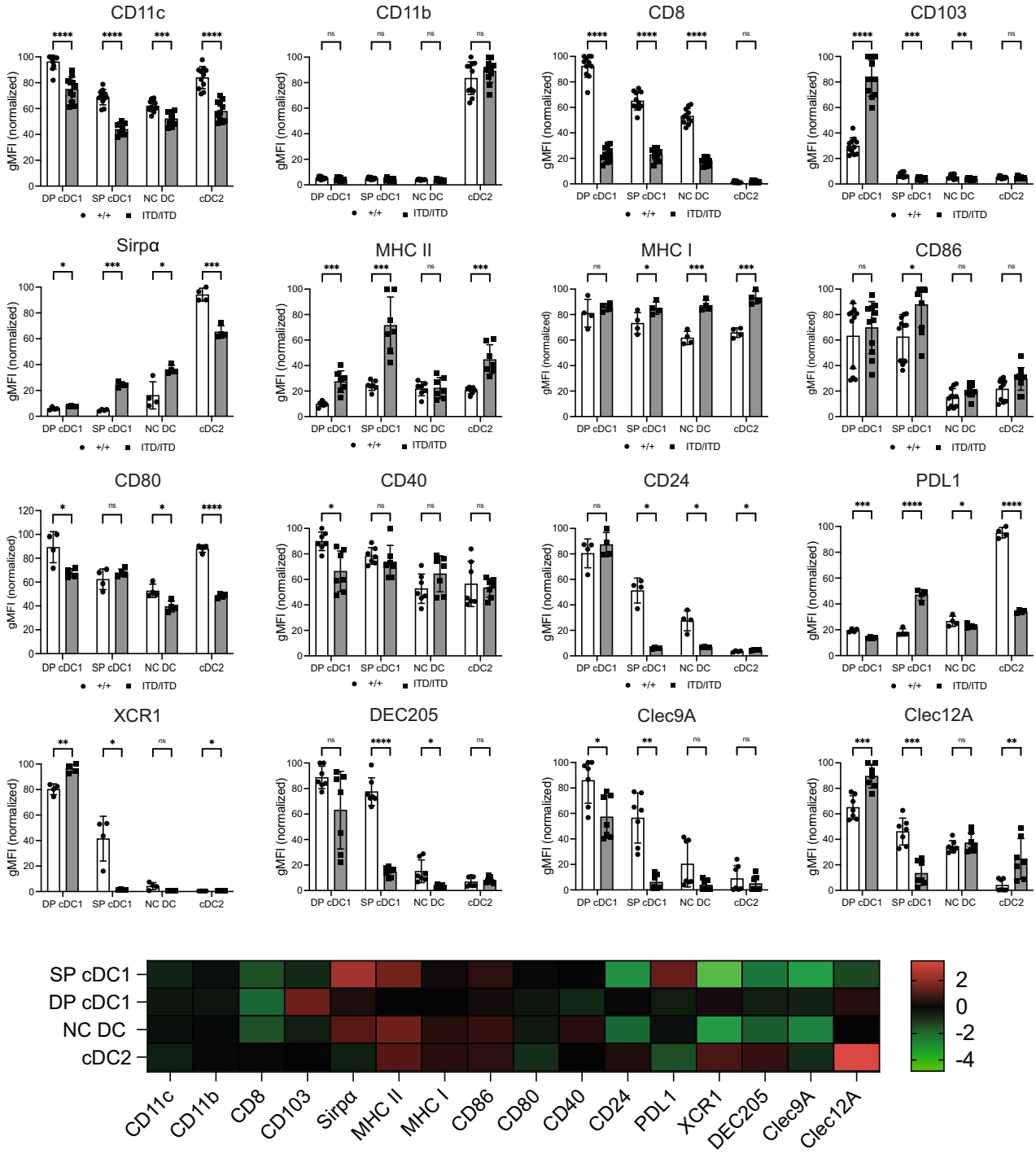

Figure 3. Flt3-ITD alters splenic DC surface expression. $Flt3^{+/+}$ (white bars) and $Flt3^{ITD/ITD}$ (gray bars) splenic cDCs were stained for surface markers and analyzed by flow cytometry. gMFI has been normalized to the maximum gMFI signal. Data are pooled from at least two independent experiments, with symbols representing individual mice. Bars are mean ± SD, multiple unpaired *t*-tests with Holm-Sidak multiple comparisons test. $^{****}P < 0.0001$; $^{***}P < 0.001$; $^{**}P < 0.01$; $^{*}P < 0.05$, ns not significant. Heat map of surface marker expression of spleen cDC1 or cDC2 isolated from $Flt3^{+/+}$ and $Flt3^{ITD/ITD}$ mice. The $\log_2$ ratio of mean gMFI of $Flt3^{ITD/ITD}$ cells relative to mean gMFI of $Flt3^{+/+}$ cells is shown. Data are pooled from at least two independent experiments.

efficiently degrade it. Therefore, antigen uptake, endosomal pH and proteolysis were assessed. Ideally, DP, NC and SP cDC1 would be isolated for both $Flt3^{+/+}$ and $Flt3^{ITD/ITD}$ mice. The low number of cDC1 subpopulations in $Flt3^{+/+}$ mice, however, meant this was not feasible. Therefore, $Flt3^{ITD/ITD}$ DP, NC and SP cDC1 were compared with $Flt3^{+/+}$ cDC1, and $Flt3^{ITD/ITD}$ cDC2 were compared with $Flt3^{+/+}$ cDC2. First, the antigen uptake was examined. cDCs were incubated with OVA-Cy5 for 15 and 90 min or dextran-A647 for 15 min and the intracellular fluorescence determined by flow cytometry. Overall, similar uptake of either OVA protein or dextran was observed for $Flt3^{+/+}$ and $Flt3^{ITD/ITD}$ cDC1 populations, although $Flt3^{ITD/ITD}$ DP cDC1 showed a trend towards reduced uptake compared with the other subsets. In contrast, OVA protein and dextran uptake by $Flt3^{ITD/ITD}$ cDC2 was elevated compared with $Flt3^{+/+}$ cDC2 (Figure 4a; Supplementary figure 4a).

To investigate $Flt3^{ITD/ITD}$ cDC2 in more detail, their ability to undertake antigen proteolysis was examined using DQ-OVA, a self-quenched form of OVA which fluoresces as it undergoes proteolysis. Purified cDCs were pulsed with DQ-OVA, excess antigen removed and cDCs examined by flow cytometry at the indicated time points. OVA-Cy5 was used to normalize for the increased uptake of DQ-OVA by $Flt3^{ITD/ITD}$ cDC2 compared with $Flt3^{+/+}$ cDC2. $Flt3^{ITD/ITD}$ cDC2 showed more rapid DQ-OVA proteolysis with the signal plateauing at 30 min compared with 60 or 90 min for $Flt3^{+/+}$ cDC2. This was accompanied by reduced endosomal pH for $Flt3^{ITD/ITD}$ cDC2 as detected by the pH sensitive probe, dextran-pHrodo, which increases fluorescence as pH decreases (Figure 4b; Supplementary figure 4b). Therefore, constitutive Flt3-ITD signaling enhances antigen uptake and proteolysis by cDC2.

Next, cytokine secretion (signal 3) by $Flt3^{+/+}$ and $Flt3^{ITD/ITD}$ cDCs was assessed. Cells were sorted to purity and equal numbers were incubated with CpG and inflammatory cytokines IFNγ and GM-CSF, conditions that elicit maximal DC IL-12 production.[36] Supernatants were harvested after 18 h and concentrations of IL-6, IL-10, IL-12p70, TNF-α and MCP-1 measured using the BD Cytometric Bead Array Assay. IL-10 and MCP-1 were not detected by cDC1 or cDC2, and IL-12 was only detected for cDC1. Robust cytokine secretion was observed for $Flt3^{+/+}$ cDC1 and $Flt3^{ITD/ITD}$ DP cDC1. In contrast, $Flt3^{ITD/ITD}$ NC cDC1 produced significantly reduced IL-6, TNF-α and IL-12 in comparison with other cDC1 subsets. Similarly, $Flt3^{ITD/ITD}$ SP cDC1 produced reduced TNF-α and IL-12 (Figure 4d). For cDC2, $Flt3^{ITD/ITD}$ DCs produced increased IL-6 and similar TNF-α in comparison with $Flt3^{+/+}$ DC (Figure 4e).

Flt3-ITD impacts cDC antigen presentation

Next, the antigen presenting capabilities of $Flt3^{ITD/ITD}$ cDC subsets were investigated. Due to the expansion of DCs (Figure 2) and regulatory T cells in $Flt3^{+/ITD}$ mice[25] *in vitro*, rather than *in vivo*, antigen presentation assays were performed to enable direct comparisons of equal numbers of $Flt3^{+/+}$ versus $Flt3^{ITD/ITD}$ cDCs in the absence of an altered extracellular environment. Spleens were harvested and cDCs isolated by sorting to purity by flow cytometry. cDCs were incubated with CellTrace-Violet (CTV)-labeled OT-I (Figure 5a) or OT-II (Figure 5b) cells in the presence of cell-associated OVA (splenocytes pulsed with OVA protein) or OVA protein alone. T cell proliferation was determined three days later. cDC1 subsets cross-present cell-associated OVA[37] whereas both cDC1 and cDC2 are capable of cross-presenting OVA protein *in vitro*.[38] A significant defect in cross-presentation of cell-associated OVA was observed for $Flt3^{ITD/ITD}$ NC cDC1 in comparison with $Flt3^{+/+}$ cDC1, while only minor changes were observed for MHC I presentation of OVA protein (Figure 5a). In contrast, Flt3-ITD largely improved MHC II antigen presentation for both antigens tested, with increased OT-II proliferation observed for $Flt3^{ITD/ITD}$ NC, SP and cDC2 in response to cell-associated OVA, and increased presentation of OVA protein by $Flt3^{ITD/ITD}$ NC and SP DCs (Figure 5b). Together, these data demonstrate that Flt3 signaling impacts MHC I and MHC II antigen presentation of both cell-associated and soluble OVA.

DISCUSSION

Flt3 is critical for DC development, but it is unclear how Flt3 expression and signaling impacts terminally differentiated cDCs. In this study we investigated Flt3 expression and determined how constitutive Flt3 signaling downstream as a result of the ITD mutation impacts DC number, phenotype and function.

In agreement with previous studies,[31,39] we identified Flt3 expression by WT splenic cDC and pDC populations. To our knowledge, this is the first time both surface and intracellular Flt3 protein in primary cDC1, cDC2 and pDC have been measured. Interestingly, surface Flt3 protein in pDCs migrates more slowly by SDS-PAGE than Flt3 expressed by cDC1 and cDC2. There are no described isoforms for murine Flt3. Therefore, it is unlikely that pDC express an alternative Flt3. Flt3 is N-linked glycosylated,[34,35] and the larger form observed in pDCs likely represents Flt3 that is more heavily decorated with carbohydrate moieties. While beyond the scope of this study, Flt3 glycosylation in DCs has yet to be investigated and as such further

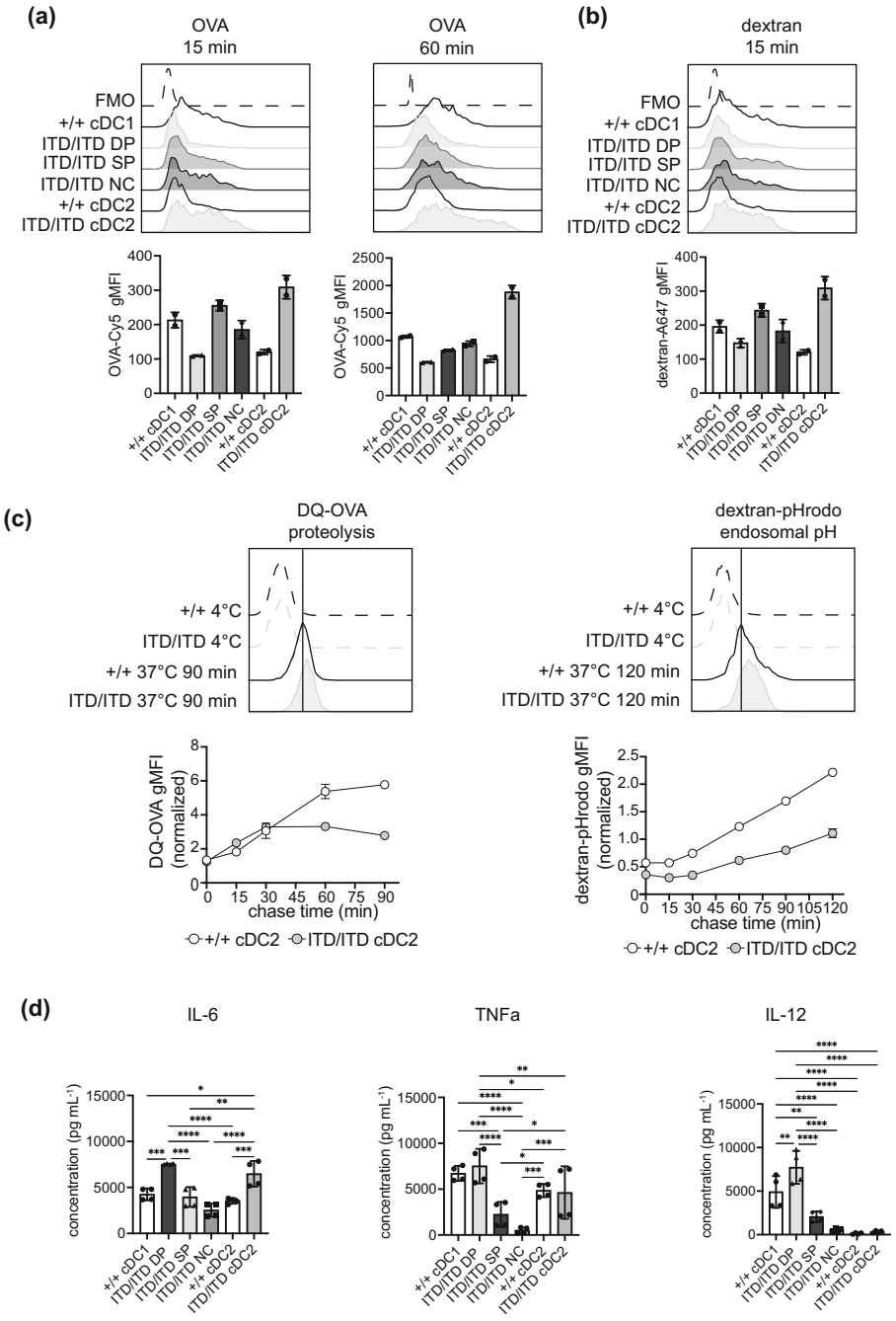

Figure 4. Flt3-ITD impacts DC function. **(a)** Purified $Flt3^{+/+}$ and $Flt3^{ITD/ITD}$ cDC1 and cDC2 populations were incubated at 37°C with 50 μg mL^{-1} OVA-Cy5 or 20 μg mL^{-1} dextran-A647 10 000 MW for the indicated times. Cells were washed and the intracellular fluorescence was determined by flow cytometry. Data are from one experiment carried out in technical duplicate and representative of two individual experiments. Bars are mean ± SD. **(b)** Purified $Flt3^{+/+}$ and $Flt3^{ITD/ITD}$ cDC2 were pulsed with 20 μg mL^{-1} DQ-OVA or 20 μg mL^{-1} dextran-pHrodo 10 000 MW for 15 min at 37°C. Cells were washed before being chased for the indicated times at 37°C. DQ-OVA and dextran-pHrodo gMFI was determined by flow cytometry. The gMFI signal for DQ-OVA or dextran-pHrodo is normalized to the OVA-Cy5 or dextran-A647 gMFI for the pulse time (15 min). Data are from one experiment carried out in technical duplicate and representative of two individual experiments. Error bars are ± SD. **(c)** $Flt3^{+/+}$ and $Flt3^{ITD/ITD}$ splenic cDC1 and cDC2 populations were isolated and cell sorted to purity. Equal numbers of cells were incubated with 0.5 μM CpG, 50 ng mL^{-1} IFNγ and 20 ng mL^{-1} GM-CSF. Supernatants were collected 18 h later, and cytokine secretion determined using BD™ Cytometric Bead Array (CBA) Mouse Inflammation Kit. Data are pooled from two independent experiments, carried out in duplicate. Bars are mean ± SD, one-way ANOVA with Dunnett's multiple comparisons test. ****$P < 0.0001$; ***$P < 0.001$; **$P < 0.01$; *$P < 0.05$, ns not significant.

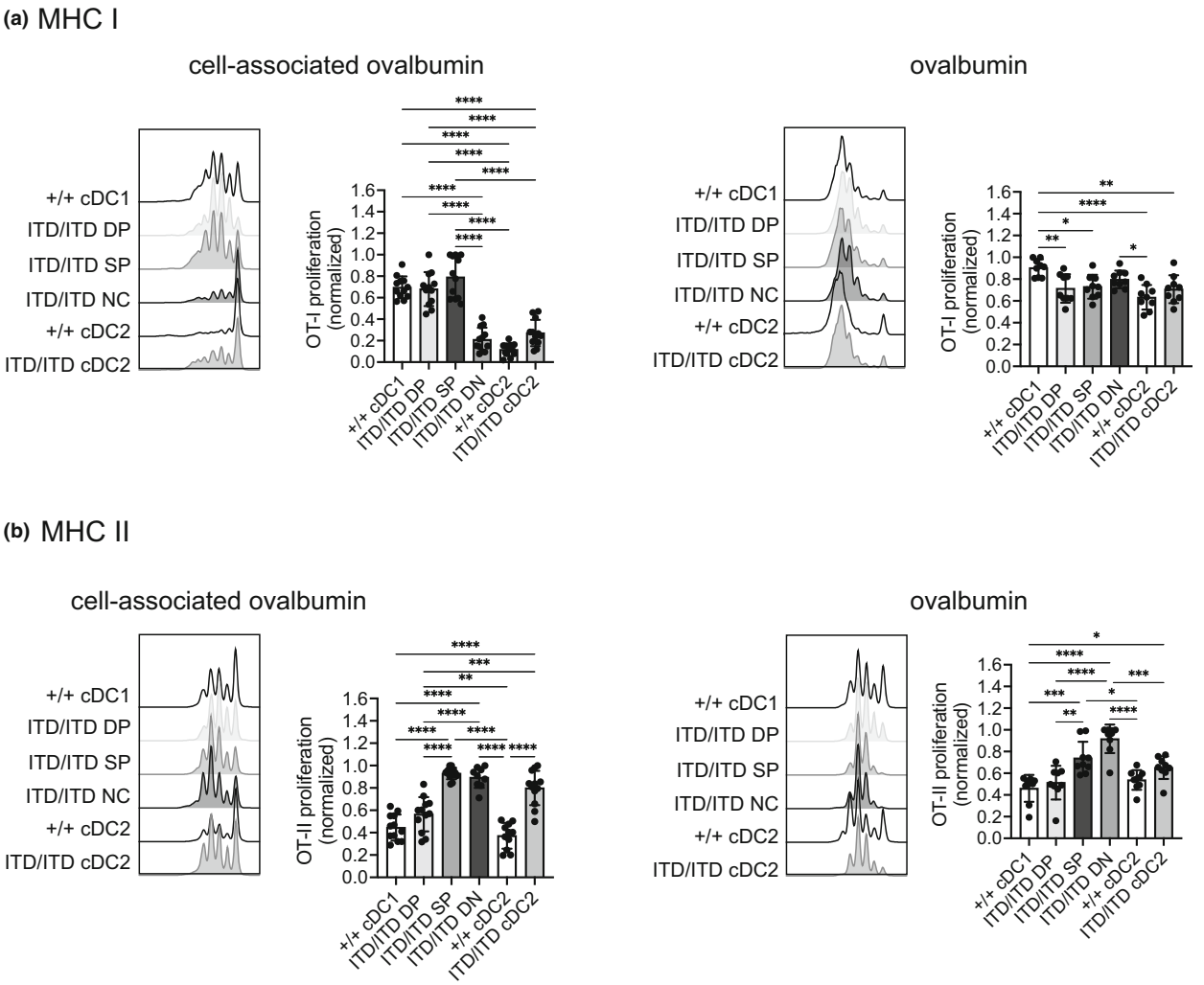

Figure 5. Flt3-ITD impacts cDC antigen presentation. Equal numbers of purified $Flt3^{+/+}$ and $Flt3^{ITD/ITD}$ cDC populations were incubated with purified CellTrace Violet (CTV)-labeled **(a)** OT-I or **(b)** OT-II cells in the presence of ovalbumin (OVA)-coated splenocytes (OCS) or 100 μg mL^{-1} OVA. Three days later, antigen presentation capacity was assessed by flow cytometric analysis. T cell proliferation was normalized to the maximum proliferation. Each symbol represents an individual mouse with data pooled from at least two independent experiments, displayed as mean ± SEM. ****$P < 0.0001$; ***$P < 0.001$; **$P < 0.01$, *$P < 0.05$, one-way ANOVA with Dunnett's multiple comparisons test.

investigations are required to fully characterize Flt3 in pDC.

We observed regulation of Flt3 expression during cDC activation, with increased surface Flt3 following activation *in vitro*. In contrast, surface Flt3 is reduced when splenic cDCs are activated by different inflammatory stimuli *in vivo*. It is likely the *in vivo* reduction is due to increased serum Flt3L in response to TLR stimulation[40] that engages and downregulates Flt3. Flt3/Flt3L signaling promotes the survival of terminally differentiated DCs, with increased apoptosis observed in bone marrow derived DC treated with Flt3 tyrosine-kinase inhibitors.[14] Therefore, upregulation of surface Flt3 during inflammation, as evidenced under *in vitro* conditions, likely increases cDC responsiveness to Flt3L, and promotes their survival and immunogenic potential *in vivo*.

We identified $Flt3^{ITD/ITD}$ DCs undergoing Flt3L-independent Flt3 signaling. This correlated with increased numbers of splenic cDC and pDC populations in $Flt3^{ITD/ITD}$ mice. In agreement with previous studies,[25] the largest expansion was NC cDC1. This differs with Flt3L administration to $Flt3^{+/+}$ mice, which expands canonical cDC1 populations.[25,26] While previous studies

have assessed the transcriptional profiles of DC populations in Flt3-ITD mice,[25] the functional consequences have not been previously examined. Our data demonstrate that constitutive Flt3 signaling downstream of Flt3-ITD leads to aberrant splenic DC phenotype and function. Elevated MHC II surface expression was observed on $Flt3^{ITD/ITD}$ DC (except NC cDC1). Similarly, $Flt3^{ITD/ITD}$ NC cDC1 and cDC2 displayed increased surface MHC I. $Flt3^{ITD/ITD}$ cDC2 exhibited increased antigen uptake, more rapid antigen proteolysis and more rapid antigen access to acidic, proteolytic intracellular compartments. These changes culminated in improved MHC II presentation of cell-associated antigen, but not soluble antigen, by these cells. Flt3-ITD promotes basal autophagy in cancer cell lines (non-DC) and Flt3-ITD^+ patient samples, while inhibition or knockdown of Flt3-ITD reduces autophagic flux.[41] This may account for elevated $CD4^+$ T cell priming since LC3-associated phagocytosis (LAP) and autophagy contribute to MHC II presentation[42]. Future experiments investigating autophagy in $Flt3^{ITD/ITD}$ DCs are of interest, particularly given its role in cDC antigen presentation.[43,44]

Our investigation of how constitutive Flt3 signaling impacts DC antigen presentation outcomes identified that MHC I cross-presentation of both cell-associated and soluble OVA was largely unchanged for $Flt3^{ITD/ITD}$ DC subsets, with the exception of NC cDC1. Here we show $Flt3^{ITD/ITD}$ NC cDC1 cannot cross-present cell-associated OVA but are capable of cross-presenting soluble OVA. To date, the immunological function of NC cDC1s is elusive. These cells were initially considered DC progenitors.[29] More recent analysis, however, renders this unlikely.[30] Human NC cDC1s can stimulate allogenic T cells[28–30] and they accumulate with pDC in influenza-infected lung.[30] Our analysis, in agreement with others,[26,30] shows $Flt3^{ITD/ITD}$ NC cDC1s have impaired IL-12 production. This may stem from reduced surface DEC205 which would render them less responsive to CpG.[45] The rare frequency of $Flt3^{+/+}$ NC cDC1s means our analysis does not permit us to conclude whether these are intrinsic functions of NC cDC1 or whether the cells are displaying altered function due to constitutive Flt3-ITD signaling.

In conclusion, we have demonstrated that splenic primary DCs regulate Flt3 and are responsive to Flt3L. Constitutive Flt3 signaling, due to the Flt3-ITD mutation, leads to significant changes to splenic DC populations with the development of cDCs that have an altered phenotype, including increased MHC expression, pro-inflammatory cytokine secretion and improved MHC II antigen presentation of cell-associated antigen. These data highlight the impact of Flt3 signaling on DC biology which is of particular interest given the increasing use of Flt3L as an adjuvant in settings of vaccination and immunotherapy. In addition, this research assists in characterizing the phenotype and function of DCs in patients that express the Flt3-ITD mutation and to assess their contribution to leukemogenesis.

METHODS

Mice

C57BL/6JArc, B6.CH-2^{bm-1} (BM-1), OT-II[46] x Ly5.1 and OT-I[47] x Ly5.1, $Flt3^{ITD/ITD}$,[21] and $IA\alpha^{-/-}$ mice[48] were used at 6–12 weeks of age. All mice were bred and maintained in specific pathogen-free conditions at the Melbourne Bioresources Platform at Bio21 Molecular Science and Biotechnology Institute. Experimental procedures were approved by the Animal Ethics Committee of the University of Melbourne (Protocol no. 1714375).

Isolation of immune cells

Primary spleen DCs were isolated as described previously.[49] In brief, organs were finely chopped and digested in the presence of DNase I (Roche) and collagenase type 3 (Worthington Biochemicals). Intercellular clusters were disrupted by the addition of 10 mM EDTA. Light density cells were isolated by density gradient separation in 1.077 g/cm^3 Nycodenz (Nycomed Pharma). Upper fractions were collected, washed and subjected to further enrichment by resuspending in a depletion cocktail containing the following rat anti-mouse mAbs specific for: CD3 (KT3-1.1), CD90 (T24/31.7), red blood cells (Ter119), B220 (RA3-6B2), Ly6G (IA8). For purification of plasmacytoid DC, the upper fractions were incubated with rat anti-mouse mAbs specific for CD3 (KT3-1.1), Thy1 (T24/31.7), red blood cells (Ter119), Ly6G (IA8) and CD19 (ID3). Cells were incubated with antibodies, washed and incubated with BioMag anti-rat IgG-coupled magnetic beads (Qiagen). The DC-enriched supernatant was recovered by magnetic separation. Where required, DCs were sorted to purity by flow cytometry on a Becton Dickinson Influx (Murdoch Children's Research Institute Flow Cytometry and Imaging Facility). cDC1 were defined as $CD11c^+$ $CD8^+$ $CD11b^-$; cDC2: $CD11c^+$ $CD8^-$ $CD11b^+$; double positive cDC1 (DP cDC1): $CD11c^+$ $CD8^+$ $CD11b^-$ $CD103^+$ $CD86^+$; double negative cDC1 (DN cDC1): $CD11c^+$ $CD8^+$ $CD11b^-$ $CD103^-$ $CD86^-$; or single positive cDC1 (SP cDC1): $CD11c^+$ $CD8^+$ $CD11b^-$ $CD103^+$ $CD86^+$.

For T cell isolation, single cell suspensions were generated from lymph nodes. Cells were stained with rat anti-mouse mAbs specific for: CD11b (M1/70), F4/80 (F4/80), red blood cells (TER119), Ly6G/-Ly6C (RB68C5), MHCII (M5/114), CD45R (RA36B2) and CD4 (GK1.5) for $CD8^+$ T cells or CD8 (53–6.7) for $CD4^+$ cells. Cells were washed and incubated with BioMag anti-rat IgG-coupled magnetic beads (Qiagen). After

magnetic depletion, the $CD4^+$ or $CD8^+$ T cell-enriched supernatant was recovered. Purity, determined by flow cytometry, was > 90%.

For B cell isolation, single cell suspensions were generated from spleens. Cells were resuspended in EDTA-BSS medium 2% (v/v) FCS and gradient centrifugation was carried out with Ficoll-Paque™ PLUS (GE Healthcare). Mononuclear cells were isolated and negative selection was carried out by incubating the cells with FITC-conjugated antibodies against CD4 (GK1.5), Ly76 (TER119) and CD43 (S7). The cells were washed and incubated with anti-FITC microbeads (Miltenyi Biotec). The B cell enriched supernatant was collected after separation with LS magnetic columns (Miltenyi Biotec). Purity, determined by flow cytometry, was > 90%.

Cells were stained with mAbs specific for CD8α (53–6.7), CD11b (M1/70), CD11c (N418), CD19 (6D5), CD24 (M1/69), CD40 (FGK45.5), CD45R/B220 (RA3-6B2), CD80 (16-10A1), CD86 (GL1), CD135/Flt3 (A2F10), CD172 (Sirpα), CD205/DEC205 (NLDC-145), CD274/PD-L1 (10F.9G2), CD317/BST2 (927), CD370/Clec9A (7H11), H-2Kb (AF6-8815), IgD (11-26c.2a), IgM (RMM-1), SiglecH (551), XCR1 (ZET) (all BioLegend). To obtain absolute cell numbers, an internal microsphere counting standard (BD Biosciences) was used. Analysis was performed with a Becton Dickinson LSRFortessa, FlowJo and Graphpad Prism software.

Immunoprecipitation

cDCs from wild type (+/+), heterozygote (+/ITD) or homozygote (ITD/ITD) littermates were isolated and stimulated in 100 ng mL^{-1} Flt3L in complete RPMI at 37°C and 10% CO_2 for 0, 10 or 30 min. Cells were washed and lysed in 0.5% NP-40, 50 mM Tris–HCl pH 7.4, 5 mM $MgCl_2$ and cOmplete™ protease inhibitor cocktail (Roche). The lysate was pre-cleared with protein G-sepharose beads (WEHI Antibody Facility) and normal rat and mouse serum (WEHI Antibody Facility). Flt3 was precipitated with anti-Flt3 (AF768, R&D Systems) antibody and protein-G sepharose beads. Proteins were eluted with reducing SDS sample buffer and analyzed by SDS-PAGE and immunoblotting.

Immunoblotting

Immune populations were isolated as described previously and the cells were lysed in 0.5% NP-40, 50 mM Tris–HCl pH 7.4, 5 mM $MgCl_2$ and cOmplete™ protease inhibitor cocktail (Roche). Post-nuclear lysates were resolved by SDS-PAGE using 8% Bolt Bis-Tris Mini Protein Gels (Invitrogen) and proteins were transferred to Immunoblot PVDF membranes (Bio-Rad). Membranes were stained with primary antibodies against Flt3 (AF768, R&D Systems), phosphorylated tyrosine (4G10, Sigma-Aldrich), actin (A5060, Sigma-Aldrich) or tubulin (DM1A, Abacm) followed by HRP-conjugated secondary antibodies.

cDC activation

For *in vitro* activation assays, cDCs were isolated and incubated overnight in complete RPMI with or without 0.5 μM CpG 1668 ODN (Bioneer) at 37°C or 4°C. For *in vivo* activation assays, mice were injected intravenously with 0.2 μM CpG, 3 μg LPS, 50 μg polyinosinic:polycytidylic acid (poly I:C) or PBS.

cDC cytokine secretion

Splenic cDC populations were isolated and cell sorted to purity. 1×10^5 cells were incubated in the presence of 0.5 μM CpG, 50 ng mL^{-1} interferon gamma (Peprotech) and 20 ng mL^{-1} granulocyte-macrophage colony-stimulating factor (GM-CSF, Peprotech). Supernatants were collected 18 h later and stored at −20°C. Cytokine secretion was determined using the BD Cytometric Bead Array Mouse Inflammation kit according to the manufacturer's instructions (BD Biosciences).

In vitro antigen presentation assay

Single cell suspensions were generated from lymph nodes of OT-I or OT-II mice and T cells were purified as described previously. Cells were washed with PBS 0.1% bovine serum albumin (BSA) and labeled with CellTrace Violet (CTV). Splenic wild type or ITD/ITD DC populations were isolated and cell sorted to purity as described previously. For antigen presentation with soluble OVA, 2.5×10^4 cDCs were incubated with 100 μg mL^{-1} OVA (Worthington Biochemical) and 0.5 μM CpG at 37°C 10% CO_2. Cells were washed extensively before plating with 5×10^4 OT-I or OT-II cells in complete RPMI and 20 ng mL^{-1} GM-CSF (Peprotech). For OVA-coated splenocytes, single cell suspensions were generated from BM-1 (for OT-I) or $IA\alpha^{-/-}$ (for OT-II) mice. Red blood cells were lysed and splenocytes were incubated with 10 mg mL^{-1} ovalbumin (Sigma) in KDS-RPMI at 37°C for 10 min. Cells were washed to remove excess OVA. 2×10^5 OVA-coated splenocytes were incubated with 2.5×10^4 cDCs and 5×10^4 OT-I or OT-II cells in complete RPMI and 20 ng mL^{-1} GM-CSF (Peprotech). For both soluble OVA and OVA-coated splenocytes, cells were incubated for 3 days and stained with mAbs specific for CD8 (53–6.7, BioLegend) or CD4 (GK1.5; Walter and Eliza Hall Antibody Facility). The number of divided OT-II and OT-I was determined as the number of $CD4^+$ or $CD8^+$ $Ly5.1^+$ cells that had undergone CTV dilution. To obtain absolute cell numbers, an internal microsphere counting standard (BD Biosciences) was used.

Antigen uptake, proteolysis and endosomal pH analyses

To assess antigen uptake, 5×10^4 purified cDCs were incubated with 50 μg mL^{-1} OVA-Cy5 in complete medium for 0–90 min at 37°C. cDCs were washed and the fluorescence measured by flow cytometry. As a control, cDCs

were pulsed with OVA-Cy5 for 90 min at 4°C. To assess antigen proteolysis and endosomal pH, 2.5×10^5 purified cDCs were incubated with 20 μg mL^{-1} DQ-OVA (Life Technologies) or dextran-pHrodo for 15 min at 37°C. Cells were washed, resuspended in complete RPMI and chased for the indicated time. At each time point, the cells were kept on ice and the fluorescence was measured by flow cytometry. As a control, cDCs were pulsed with DQ-OVA or dextran-pHrodo for 15 min at 4°C. The signal was calculated for the 37°C chase time point by subtracting the MFI at 4°C.

ACKNOWLEDGMENTS

The authors acknowledge critical evaluation of the manuscript by P Beavis, S Naik and C Audiger. This work was supported by Department of Health Australia, National Health and Medical Research Council grants or fellowships 1058193, 1113293, 1154502 and 1163090 (to JAV) and 1161101 and 1129672 (to JDM), Department of Education and Training, Australian Research Council (ARC) grants or fellowships 160103134, 170102471 and 190102213 (to JAV) and 190101242, 180100844, 160101373 and 180100521 (to JDM), a Human Frontiers Science Program grant (0064/2011 to JAV), and the Australian Government's National Health and Medical Research Council Victorian State Government Operational Infrastructure Support and the Independent Research Institutes Infrastructure Support Scheme. Open access publishing facilitated by The University of Melbourne, as part of the Wiley ? The University of Melbourne agreement via the Council of Australian University Librarians.

AUTHOR CONTRIBUTIONS

Kayla R Wilson: Conceptualization; investigation; formal analysis; methodology; writing – original draft; writing – review and editing. **Christophe Macri:** Investigation; formal analysis. **Jose A Villadangos:** Conceptualization; funding acquisition; supervision; writing – review and editing. **Justine D Mintern:** Conceptualization; funding acquisition; project administration; supervision; writing – review and editing.

CONFLICT OF INTEREST

The authors declare no conflict of interest.

REFERENCES

1. Saito Y, Boddupalli CS, Borsotti C, Manz MG. Dendritic cell homeostasis is maintained by nonhematopoietic and T-cell-produced Flt3-ligand in steady state and during immune responses. *Eur J Immunol* 2013; **43**: 1651–1658.
2. Zhang S, Mantel C, Broxmeyer HE. Flt3 signaling involves tyrosyl-phosphorylation of SHP-2 and SHIP and their association with Grb2 and Shc in Baf3/Flt3 cells. *J Leukoc Biol* 1999; **65**: 372–380.
3. Sathaliyawala T, O'Gorman WE, Greter M, *et al.* Mammalian target of rapamycin controls dendritic cell development downstream of Flt3 ligand signaling. *Immunity* 2010; **33**: 597–606.
4. Laouar Y, Welte T, Fu XY, Flavell RA. STAT3 is required for Flt3L-dependent dendritic cell differentiation. *Immunity* 2003; **19**: 903–912.
5. Onai N, Obata-Onai A, Tussiwand R, Lanzavecchia A, Manz MG. Activation of the Flt3 signal transduction cascade rescues and enhances type I interferon-producing and dendritic cell development. *J Exp Med* 2006; **203**: 227–238.
6. Maraskovsky E, Brasel K, Teepe M, *et al.* Dramatic increase in the numbers of functionally mature dendritic cells in Flt3 ligand-treated mice: multiple dendritic cell subpopulations identified. *J Exp Med* 1996; **184**: 1953–1962.
7. Waskow C, Liu K, Darrasse-Jeze G, *et al.* The receptor tyrosine kinase Flt3 is required for dendritic cell development in peripheral lymphoid tissues. *Nat Immunol* 2008; **9**: 676–683.
8. Maraskovsky E, Daro E, Roux E, *et al. In vivo* generation of human dendritic cell subsets by Flt3 ligand. *Blood* 2000; **96**: 878–884.
9. Pulendran B, Banchereau J, Burkeholder S, *et al.* Flt3-ligand and granulocyte colony-stimulating factor mobilize distinct human dendritic cell subsets *in vivo*. *J Immunol* 2000; **165**: 566–572.
10. Mackarehtschian K, Hardin JD, Moore KA, Boast S, Goff SP, Lemischka IR. Targeted disruption of the flk2/flt3 gene leads to deficiencies in primitive hematopoietic progenitors. *Immunity* 1995; **3**: 147–161.
11. McKenna HJ, Stocking KL, Miller RE, *et al.* Mice lacking flt3 ligand have deficient hematopoiesis affecting hematopoietic progenitor cells, dendritic cells, and natural killer cells. *Blood* 2000; **95**: 3489–3497.
12. Ginhoux F, Liu K, Helft J, *et al.* The origin and development of nonlymphoid tissue $CD103^+$ DCs. *J Exp Med* 2009; **206**: 3115–3130.
13. Lyman SD, Seaberg M, Hanna R, *et al.* Plasma/serum levels of flt3 ligand are low in normal individuals and highly elevated in patients with Fanconi anemia and acquired aplastic anemia. *Blood* 1995; **86**: 4091–4096.
14. Whartenby KA, Calabresi PA, McCadden E, *et al.* Inhibition of FLT3 signaling targets DCs to ameliorate autoimmune disease. *Proc Natl Acad Sci USA* 2005; **102**: 16741–16746.
15. Cueto FJ, Del Fresno C, Brandi P, *et al.* DNGR-1 limits Flt3L-mediated antitumor immunity by restraining tumor-infiltrating type I conventional dendritic cells. *J Immunother Cancer* 2021; **9**: e002054.
16. Wilson KR, Villadangos JA, Mintern JD. Dendritic cell Flt3 – regulation, roles and repercussions for immunotherapy. *Immunol Cell Biol* 2021; **99**: 962–971.

17. Hayakawa F, Towatari M, Kiyoi H, *et al.* Tandem-duplicated Flt3 constitutively activates STAT5 and MAP kinase and introduces autonomous cell growth in IL-3-dependent cell lines. *Oncogene* 2000; **19**: 624–631.
18. Mizuki M, Fenski R, Halfter H, *et al.* Flt3 mutations from patients with acute myeloid leukemia induce transformation of 32D cells mediated by the Ras and STAT5 pathways. *Blood* 2000; **96**: 3907–3914.
19. Kiyoi H, Ohno R, Ueda R, Saito H, Naoe T. Mechanism of constitutive activation of FLT3 with internal tandem duplication in the juxtamembrane domain. *Oncogene* 2002; **21**: 2555–2563.
20. Choudhary C, Schwable J, Brandts C, *et al.* AML-associated Flt3 kinase domain mutations show signal transduction differences compared with Flt3 ITD mutations. *Blood* 2005; **106**: 265–273.
21. Lee BH, Tothova Z, Levine RL, *et al.* FLT3 mutations confer enhanced proliferation and survival properties to multipotent progenitors in a murine model of chronic myelomonocytic leukemia. *Cancer Cell* 2007; **12**: 367–380.
22. Nagel G, Weber D, Fromm E, *et al.* Epidemiological, genetic, and clinical characterization by age of newly diagnosed acute myeloid leukemia based on an academic population-based registry study (AMLSG BiO). *Ann Hematol* 2017; **96**: 1993–2003.
23. Yokota S, Kiyoi H, Nakao M, *et al.* Internal tandem duplication of the FLT3 gene is preferentially seen in acute myeloid leukemia and myelodysplastic syndrome among various hematological malignancies. A study on a large series of patients and cell lines. *Leukemia* 1997; **11**: 1605–1609.
24. Papaemmanuil E, Gerstung M, Bullinger L, *et al.* Genomic classification and prognosis in acute myeloid leukemia. *N Engl J Med* 2016; **374**: 2209–2221.
25. Lau CM, Nish SA, Yogev N, Waisman A, Reiner SL, Reizis B. Leukemia-associated activating mutation of Flt3 expands dendritic cells and alters T cell responses. *J Exp Med* 2016; **213**: 415–431.
26. Bar-On L, Birnberg T, Lewis KL, *et al.* CX_3CR1^+ $CD8\alpha^+$ dendritic cells are a steady-state population related to plasmacytoid dendritic cells. *Proc Natl Acad Sci USA* 2010; **107**: 14745–14750.
27. Caminchi I, Vremec D, Ahmet F, *et al.* Antibody responses initiated by Clec9A-bearing dendritic cells in normal and $Batf3^{-/-}$ mice. *Mol Immunol* 2012; **50**: 9–17.
28. Villani AC, Satija R, Reynolds G, *et al.* Single-cell RNA-seq reveals new types of human blood dendritic cells, monocytes, and progenitors. *Science* 2017; **356**: eaah4573.
29. See P, Dutertre CA, Chen J, *et al.* Mapping the human DC lineage through the integration of high-dimensional techniques. *Science* 2017; **356**: eaag3009.
30. Leylek R, Alcantara-Hernandez M, Lanzar Z, *et al.* Integrated cross-species analysis identifies a conserved transitional dendritic cell population. *Cell Rep* 2019; **29**: e3738.
31. Miller JC, Brown BD, Shay T, *et al.* Deciphering the transcriptional network of the dendritic cell lineage. *Nat Immunol* 2012; **13**: 888–899.
32. Teshima T, Reddy P, Lowler KP, *et al.* Flt3 ligand therapy for recipients of allogeneic bone marrow transplants expands host $CD8\alpha^+$ dendritic cells and reduces experimental acute graft-versus-host disease. *Blood* 2002; **99**: 1825–1832.
33. O'Keeffe M, Brodnicki TC, Fancke B, *et al.* Fms-like tyrosine kinase 3 ligand administration overcomes a genetically determined dendritic cell deficiency in NOD mice and protects against diabetes development. *Int Immunol* 2005; **17**: 307–314.
34. Lyman SD, James L, Zappone J, Sleath PR, Beckmann MP, Bird T. Characterization of the protein encoded by the flt3 (flk2) receptor-like tyrosine kinase gene. *Oncogene* 1993; **8**: 815–822.
35. Schmidt-Arras DE, Bohmer A, Markova B, Choudhary C, Serve H, Bohmer FD. Tyrosine phosphorylation regulates maturation of receptor tyrosine kinases. *Mol Cell Biol* 2005; **25**: 3690–3703.
36. Hochrein H, O'Keeffe M, Luft T, *et al.* Interleukin (IL)-4 is a major regulatory cytokine governing bioactive IL-12 production by mouse and human dendritic cells. *J Exp Med* 2000; **192**: 823–833.
37. Schnorrer P, Behrens GM, Wilson NS, *et al.* The dominant role of $CD8^+$ dendritic cells in cross-presentation is not dictated by antigen capture. *Proc Natl Acad Sci USA* 2006; **103**: 10729–10734.
38. Theisen DJ, Davidson JT 4th, Briseno CG, *et al.* WDFY4 is required for cross-presentation in response to viral and tumor antigens. *Science* 2018; **362**: 694–699.
39. Kingston D, Schmid MA, Onai N, Obata-Onai A, Baumjohann D, Manz MG. The concerted action of GM-CSF and Flt3-ligand on *in vivo* dendritic cell homeostasis. *Blood* 2009; **114**: 835–843.
40. Eidenschenk C, Crozat K, Krebs P, *et al.* Flt3 permits survival during infection by rendering dendritic cells competent to activate NK cells. *Proc Natl Acad Sci USA* 2010; **107**: 9759–9764.
41. Heydt Q, Larrue C, Saland E, *et al.* Oncogenic FLT3-ITD supports autophagy via ATF4 in acute myeloid leukemia. *Oncogene* 2018; **37**: 787–797.
42. Roche PA, Furuta K. The ins and outs of MHC class II-mediated antigen processing and presentation. *Nat Rev Immunol* 2015; **15**: 203–216.
43. Mintern JD, Macri C, Chin WJ, *et al.* Differential use of autophagy by primary dendritic cells specialized in cross-presentation. *Autophagy* 2015; **11**: 906–917.
44. Mintern JD, Villadangos JA. Autophagy and mechanisms of effective immunity. *Front Immunol* 2012; **3**: 60.
45. Lahoud MH, Ahmet F, Zhang JG, *et al.* DEC-205 is a cell surface receptor for CpG oligonucleotides. *Proc Natl Acad Sci USA* 2012; **109**: 16270–16275.
46. Barnden MJ, Allison J, Heath WR, Carbone FR. Defective TCR expression in transgenic mice constructed using cDNA-based α- and β-chain genes under the control of heterologous regulatory elements. *Immunol Cell Biol* 1998; **76**: 34–40.

47. Hogquist KA, Jameson SC, Heath WR, Howard JL, Bevan MJ, Carbone FR. T cell receptor antagonist peptides induce positive selection. *Cell* 1994; **76**: 17–27.
48. Kontgen F, Suss G, Stewart C, Steinmetz M, Bluethmann H. Targeted disruption of the MHC class II aa gene in C57BL/6 mice. *Int Immunol* 1993; **5**: 957–964.
49. Vremec D. The isolation of mouse dendritic cells from lymphoid tissues and the identification of dendritic cell subtypes by multiparameter flow cytometry. *Methods Mol Biol* 2010; **595**: 205–229.

SUPPORTING INFORMATION

Additional supporting information may be found online in the Supporting Information section at the end of the article.